The 8th European Congress on Computational Methods in Applied Sciences and Engineering
ECCOMAS Congress 2022
5-9 June 2022, Oslo, Norway

PENALIZED DIRECT-FORCING METHOD AND POWER-LAW-BASED WALL MODEL FOR IMMERSED-BOUNDARY NUMERICAL SIMULATIONS OF OBSTACLES IN TURBULENT FLOW

IDRIS HAMADACHE[1], MICHEL BELLIARD[1] AND PIERRE SAGAUT[2]

[1] French Atomic Energy Comission (CEA)
IRESNE-DER-SESI-LEMS
Centre de Cadarache - 13108 St Paul Lez Durance
e-mail: idris.hamadache@cea.fr, michel.belliard@cea.fr

[2] Aix-Marseille Université
Laboratoire de Mécanique, Modélisation et Procédés Propres UMR CNRS 7340
Technopole de Château-Gombert 38, rue Frédéric Joliot-Curie 13451 Marseille, France
email: pierre.sagaut@univ-amu.fr

Key words: Computational Fluid Mechanics, Penalized Direct Forcing, turbulent wall model

Abstract. In this paper, academic and industrial test cases have been conducted in order to validate the approach of using a Penalized Direct Forcing method coupled with an immersed turbulent wall model. Good results are obtained compared to a body fitted mesh with the Werner & Wengle wall model. In a shortcoming second step, we can project the coupling between the immersed wall law and a K-epsilon model, as well as obstacle shape optimization during the flow computation.

1 Context

The context of this work is the design of passive safety devices acting as hydraulic diodes and, more precisely, the optimisation of the shape of their parts. Here, we are facing the computation of the fluid flow inside passive safety devices designed for French Pressurized Water Reactor (PWR) of 3rd generation. Following the Fukushima accident (loss of electrical sources), passive safety systems have gained in popularity. The added value of these systems is to reduce the dependence of nuclear power plants on active safety systems (e.g. emergency pumps powered by electrical sources) which represent a significant cost of operation and need regular maintenance. The introduction of passive safety systems allows to improve the safety of nuclear power plants while reducing their operating costs.

The systems we are studying are based on the hydraulic diode principle. One of these passive systems is the flow limiter, patented by the CEA [1]. It consists of thin fins, cleverly placed in the downcomer of a PWR vessel, at the level of the cold branch inlet

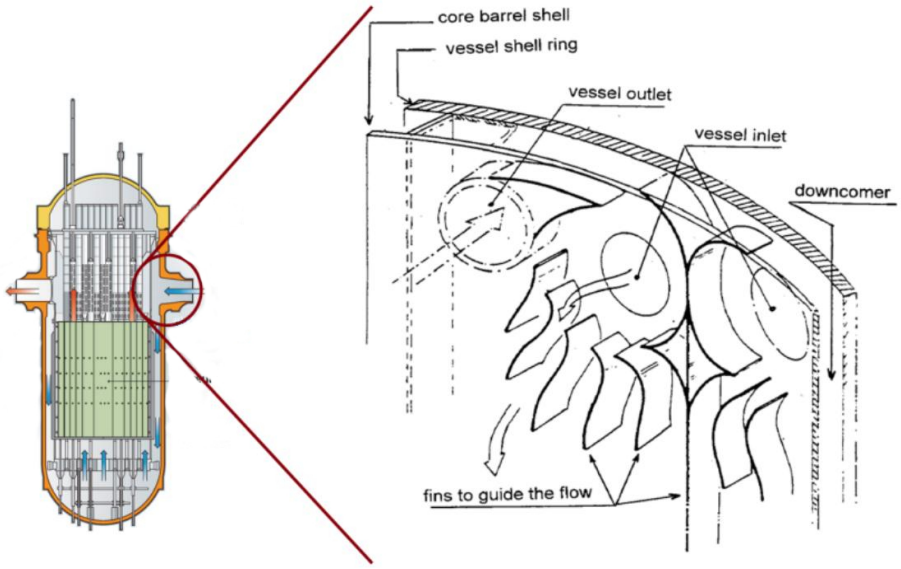

Figure 1: Illustration of the flow limiter and its location in the vessel of a PWR during normal conditions[2]

(see Figure 1). The principle consists in letting the flow pass in one direction and reduce it in the other. This flow reduction is obtained by the creation of a flow vortex induced by the presence of fins. The purpose of the limiter is therefore to not distrub the flow during normal conditions, while minimizing the flow leaving the vessel in the event of a large-break loss of coolant type accident, which could lead to the total emptying of the vessel and discovering of the core.

Aim

As mentioned in the context, our final goal is to realize a shape optimization process for the previously presented devices. This shape optimisation process led us to consider that a fictitious domain method, introduced by Saul'ev [3], is an adequate modelisation method because of its ability to dissociate the fluid domain from the obstacle one. With this approach and via immersed boundary conditions, the shape of the in-flow obstacles (as the fins in the flow limiter) can vary with no impact on the computation grid. This grant us the possibility to work on several different forms of obstacles without having to use an adapted mesh at each mesh variation. This is a great advantage that can save us time. Here, we use the Penalized Direct Forcing [4] method as immersed boundary method.

But, in order to compute turbulent flows (often with a cartesian mesh for a fictitious domain method), we need a fine enough mesh on the near wall region in order to solve the turbulent boundary layer. Doing so can be time consuming and require a higher grid

generation cost. That is why we have chosen to use an immersed turbulent wall model that will compute the shear stress and the velocity on the near wall area.

First, we will start by introducing the Penalized Direct Forcing Method, followed by the presentation of the turbulent wall model. Later, we will present results of simulation for academic and industrial test cases.

2 Fictitious domain method

With the fictitious domain methods, the physical domain is embedded in a greater domain which is used as the computation domain and called fictitious domain. In other words, fictitious domain methods consist in dissociating the physical domain from the computational domain. The mesh is no longer adapted to the shape of the physical domain and usually is a Cartesian mesh that covers the physical and external domains to become the only computational domain. The shape of the physical domain is taken into account by modifying the equations of the problem or by adding new terms. This approach has been developped by V.K. SAUL'EV [3] in the 1960s.

Implementation is greatly simplified for the engineer as it is now a matter of using a single mesh (which can be a "simple" Cartesian mesh) over the entire domain which no longer has to take into account the geometry of the obstacles.

This avoids the need to mesh each obstacle (very useful for cluttered environments or, as is the case here, shape changing object).

2.1 Penalized Direct Forcing method

M. Belliard et al. [5] have developed a new method called Penalized Direct Forcing (PDF), which is based on L^2-penalty method [6] and Direct Forcing (DF) [7]. The PDF method takes the advantages of both method by using a forcing term as for the DF method but expressed as a L^2-penalty that makes the forcing term implicit.

The forcing term is added to the momentum equation and is expressed as follows :

$$F_{PDF} = \frac{\chi_s}{\eta \cdot \delta t}(\mathbf{u}_{imp}^{n+1} - \mathbf{u}^n) \tag{1}$$

with $\eta \, \epsilon \, R_*^+$ the penalty term, as $\eta \ll 1$ and u_{imp}^{n+1} the imposed speed at the interface.

This formulation also has the advantage to be easily adaptable for a fractional-step algorithm [8]. Moreover, with the immersed boundary approach, on a discrete level, the approximation of the immersed boundary may not be located on nodes. Therefore the velocity imposed by the immersed boundary on its closest nodes (grey cross on Figure 3) has to be computed or reconstructed. It can be done either by direct assignment or by an intepolation of the velocity. More informations are given in [9]

2.2 Fractional-step method

The aim here is to compute the velocity using an implicit approximation of the imposed velocity in the forcing term. This is done by spreading the forcing term in the prediction

and the correction stages of the projection.

The first step of this fractional-step algorithm is the prediction step : it consists in computing a predicted velocity $\tilde{\mathbf{u}}$ by adding the forcing as a source term in the momentum equation, which is solved ignoring or approximating the pressure gradient :

$$\rho^n \frac{\tilde{\mathbf{u}} - \mathbf{u}^n}{\delta t} + \nabla_h \cdot \rho^n (\mathbf{u}^n \otimes \mathbf{u}^n) - \mu \nabla_h^2 \ \tilde{\mathbf{u}} \ + \nabla P^n = \frac{\chi_s \rho^n}{\eta \delta t} (\mathbf{u}_{imp}^{n+1} - \tilde{\mathbf{u}}) \ on \ \Omega \tag{2}$$

The second step of the algorithm is the correction step in order to recover the pressure P^{n+1} and the solenoïdal velocity $\mathbf{u}^{n+1}$, by using the just computed predicted velocity $\tilde{\mathbf{u}}$ and the second part of the forcing term :

$$\rho^n \frac{\mathbf{u}^{n+1} - \tilde{\mathbf{u}}}{\delta t} + \nabla_h (P^{n+1} - P^n) = \frac{\chi_s \rho^n}{\eta \delta t} (\tilde{\mathbf{u}} - \mathbf{u}^{n+1}) \ on \ \Omega \tag{3}$$

The correction equation (3) can be simplified as :

$$\rho^n (1 + \frac{\chi_s}{\eta})(\mathbf{u}^{n+1} - \tilde{\mathbf{u}}) = -\nabla_h (P^{n+1} - P^n) \ on \ \Omega \tag{4}$$

Then, we apply the divergence operator, at a space-discrete level with a finite element formulation, to the equation (4), and, with the help of the continuity equation, the previous equation becomes :

$$div(\frac{\eta}{\eta + \chi_s}) \ \nabla_h (P^{n+1} - P^n) = \frac{1}{\delta t} div(\rho^n \tilde{\mathbf{u}}) \tag{5}$$

And finally the equation (4) leads us to get the new velocity :

$$\mathbf{u}^{n+1} = \tilde{\mathbf{u}} - \frac{\delta t}{(1 + \frac{\chi_s}{\eta})\rho^n} \nabla_h (P^{n+1} - p^n) \quad on \ \Omega \tag{6}$$

3 Wall model

The graph in Figure 2, illustrates the theoretical evolution of the dimensionless velocity as a function of the dimensionless distance to the wall [11].

Here U is the tangential velocity, u^* the friction velocity and $y^+ = \frac{yu^*}{\nu}$ the dimensionless distance to the wall with ν the fluid viscosity at the wall and y the distance to the wall. The friction velocity can be defined by $\tau = \rho \cdot u^{*2}$ with τ the wall shear stress. It can be seen that, as close as possible to the wall, the dimensionless velocity $u^+ = \frac{u}{u^*}$ evolves linearly with the distance to the wall, this area is called the viscous sublayer ; this is a zone where viscous effects are predominant with a viscosity ν of the same order as the turbulent viscosity. Then starting from $y^+ = 20\text{-}30$, the evolution becomes logarithmic : this part is called the inertial zone (the viscous effects become negligible compared to the inertial effects).

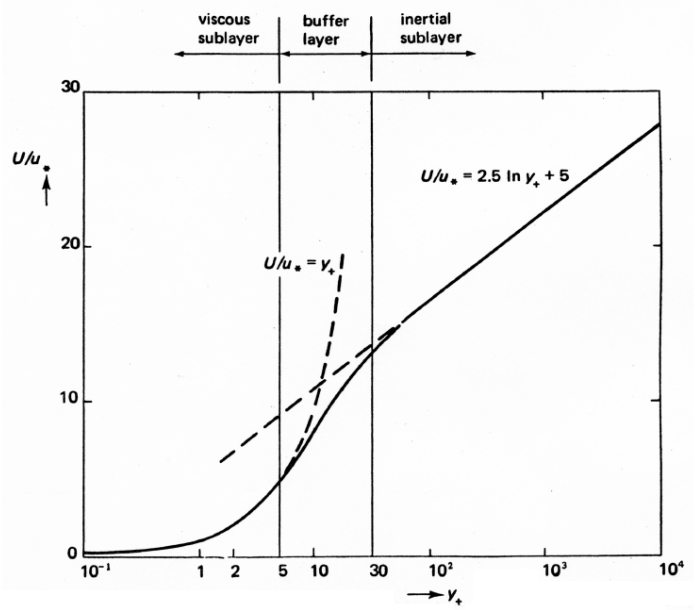

Figure 2: Diagram illustrating the evolution of the dimensionless velocity profile in the turbulent boundary layer [10].

A wall model is used to determine the velocity profile, in the vicinity of the surface of the object of study, as a function of the distance from the wall in a turbulent flow. It fills the gaps in the near-wall turbulence model when we do not want to use a very fine mesh near the boundary.

3.1 Power law wall model

Wilhelm et al. [12] proposed an another wall model with an improvement for the computation of the friction velocity. This new wall model is no more expressed in log, but in power of y^+. It allows to not rely on an iterative procedure for the computation of the friction velocity and proposes a simple technique to compute velocity at a forced node.

To reconstruct this velocity, [12] relies on the use of fluid points to determine the velocity at a reference point (Ref) which lies on the normal direction to the wall. Once the position y_{ref} and the velocity u_{ref} of the reference point are determined, the velocity at the forced node y can easily be computed : the velocity profile has two expressions, depending on whether the Ref point is in the viscous sub-layer or not :

$$If \quad y^+_{Ref} < y^+_c \quad then \quad u(y) = u_{Ref}\frac{y}{y_{Ref}} \tag{7}$$

$$If \quad y^+_{Ref} > y^+_c \quad then \quad u(y) = u_{Ref}(\frac{y}{y_{Ref}})^B \tag{8}$$

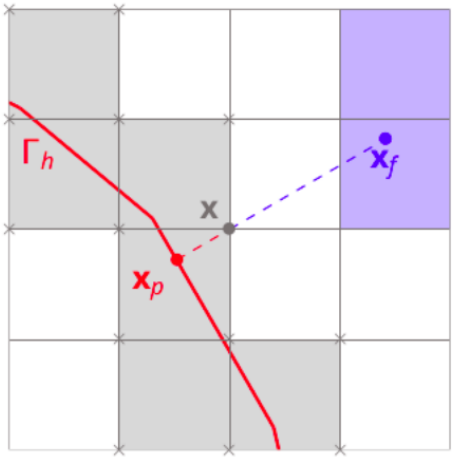

Figure 3: The grey cells are the ones crossed by the approximation of the boundary, the grey crosses are the forced nodes. The blue cells are the pure fluid cells.

with A = 8.3 and B = 1/7. The viscous sub-layer height y_c^+ is fixed to 11.81 ([12]).

This is the wall model we want to evaluate on academic and industrial test cases, in order to use it later on the shape optimization process.

3.2 Determination of the reference point at the discret level

Once the projection of the forced point (x, cf. Figure 3) on the immersed boundary (x_p) is done, we define the reference point (x_f) as the fluid point, on the normal direction, belonging to a pure fluid cell. A pure fluid cell is a cell in the near-wall fluid domain without any of its nodes being in contact with the cells crossed by the immersed boundary (blue cell in Figure 3).

4 Numerical results

4.1 An academic test case

In order to validate the approach of using a Penalized Direct Forcing method coupled with an immersed turbulent wall model [12], we have computed the turbulent flow in a plane canal as reported by Comte-Bellot [13].

The fluid is air, the length of the canal is set to 10.8 m, the distance between the planes is 0.18 m, the kinematic viscosity is : $1.5 \cdot 10^{-}5\ m^2/s$, the density set to 1.208 kg/m^3, the Reynolds number Re=104760. The RANS equations are solved with the CEA code TrioCFD, using the Penalized Direct Forcing method for the consideration of the immersed boundaries, and the experimental eddy viscosity, cf. Figure 5 left.

The exprerimental velocity field is imposed at the inlet of the canal (Figure 5 right).

Imposing that velocity field at the inlet allows us to get, in a faster way, a fully developped flow. The usage of an experimental eddy viscosity spare us the usage of a turbulence

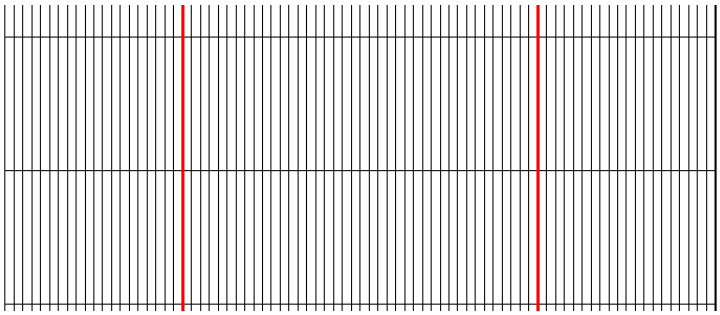

Figure 4: A sample of the fictitious domain mesh with the immersed boundary in red

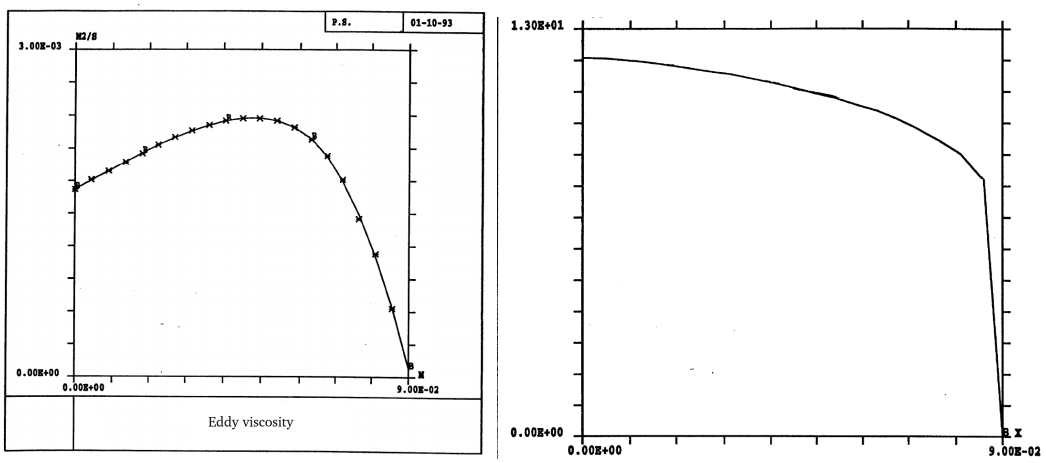

Figure 5: The eddy viscosity (left) and the inlet velocity (right) used for our study, displayed for half the distance between the two canal planes.

model and thus allows us to focus on the ability of the immersed wall model to compute the boundary node velocity.

First, we validate our immersed wall law on body fitted cases using the same y^+. To do this, the immersed boundary is located on mesh axis, cf. Figure 4.1.

A simple uniform cartesian grid is used to mesh the fictitious domain that contain the canal planes. We used several mesh sizes, along the perpendicular direction to the planes, to match the position of the first node to the following y^+ :

Cell size (m)	0,00115	0,0023	0,0035	0,0045	0,005
y^+	30	60	90	117	130

Figure 6 plots the velocity L2-norm error as a function of y^+ for the PDF method coupled with the [12] wall model (black). The classical body fitted approach with a Werner

& Wengle[14] wall model is reported in blue. We can see that the error between the PDF method with the immersed wall model is very similar to the bodyfitted with the W&W wall model, the difference is less than 2%. The y^+ convergence order is about 0.6.

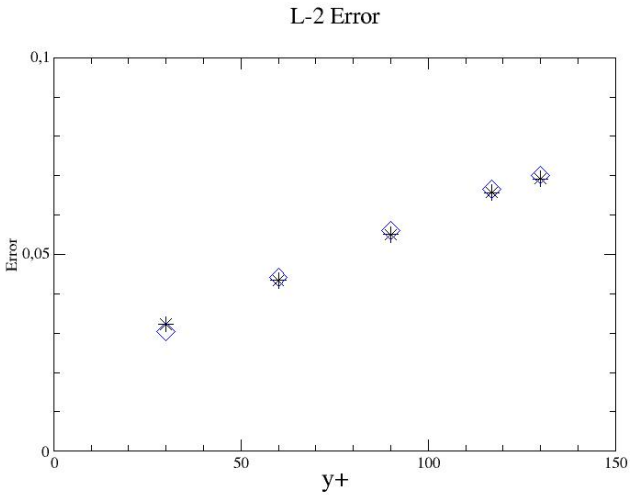

Figure 6: L2-norm error of the velocity for the PDF coupled with the wall model (black stars) and the bodyfitted (blue squares) with Werner & Wengle wall model

Second, we evaluate the error introduced by a y^+ distribution when the mesh axis is not aligned with the canal.
Then, we also did simulations with tilted canal planes to assess the error when the distance to the wall is no longuer uniform. Figure 7 plots the velocity L2-norm error as a function of y^+ for the PDF method with the [12] wall model for various angles. Four angles of inclination, $\theta = 0^o, 11^o, 30^o, 45^o$, are considered.

On Figure 7 we can see in blue (0^o) the error for the non tilted case. For an angle of 30^o or higher the error is similar to the aligned case. The error obtained for an angle of 11^o is the highest.

4.2 An industrial test case

We also computed the flow around an industrial device which is the flow limiter (Figures 8 and 9), with the following conditions : an input mass flow rate of 5200 kg/s, an ouput pressure of 43.7 bar, a constant eddy viscosity (0.141 m^2/s ; obtained via Schlichting's formula : $\nu_t = c \cdot l \cdot \rho \cdot V$ with c = 0.047, l = 0.3 m , $\rho = 795.25\ kg/m^3$ and V = 10 m/s). We used the same code (TrioCFD) and the same approach : the Penalized Direct Forcing method and immersed wall model. Similarly to the academic test case, the PDF

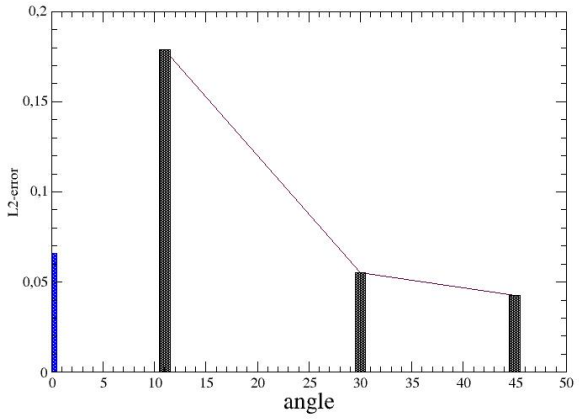

Figure 7: L-2 error for various angles of the planes

approach applied on an industrial test case, provides similar results compared to a body fitted meshing with the W&W wall model. This work shows that, with a low generation cost mesh, we can get an equivalent results than with a body fitted grid.

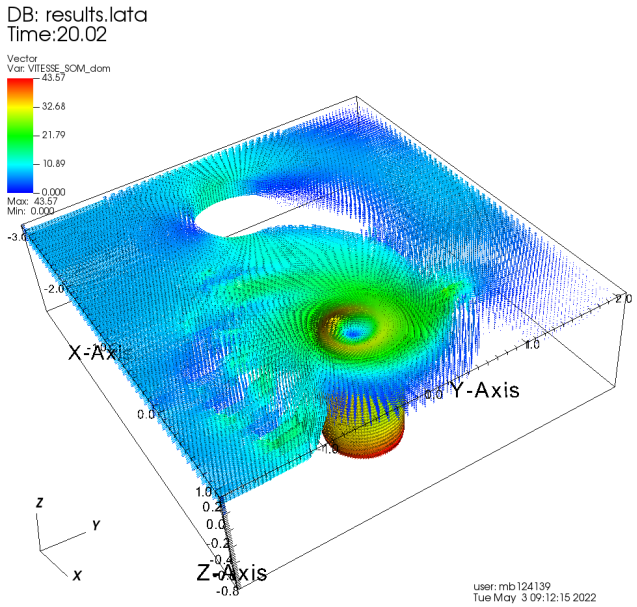

Figure 8: Simulation of the flow limiter with the Penalized Direct Forcing method and the immersed wall model

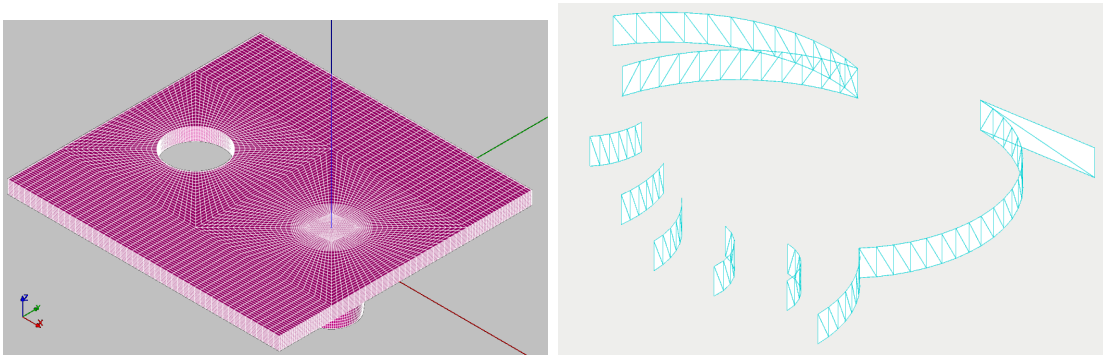

Figure 9: Mesh of the flow limiter with the PDF approach

5 Concluding remarks

We have presented the PDF method equiped with an immersed wall model, based on a power-law velocity profile for the description of the turbulent boundary layer, and its numerical implementation. This wall model was chosen because of its polynomial expression allowing freedom from an iterative procedure for the calculation of the friction velocity. At the academic level, immersed boundary simulations of the comte-Bellot experiment were conducted. Several mesh size have been used to verify the model on body-fitted mesh cases. Satisfactory results are obtained for axis aligned (y^+ constant distance to the wall) or tilted (y^+ fluctuating distance to the wall) canal planes. The y^+ convergence order is about 0.6 in relative velocity L2-norm error and the error is the highest for a small angle of dicrepency between the mesh axis and the canal one. At the Industrial level, flow simulations inside an in-vessel flow limiter were conducted to verify the feasibility of the industrial computation with turbulent immersed wall laws. Results are coherent comparing with previous laminar results [9], but with higher pressure drop. Concerning the perspectives, we can project the coupling between the immersed wall law and a K-epsilon model, as well as obstacle shape optimization during the flow computation.

6 References

[1] G.M. Gautier. Dispositif limiteur de débit inverse de fluide. patent n 88 12665. 1988.

[2] E. Stratta and M. Belliard. Thermal-hydraulic study of passive safety system based on the hydraulic diodie principle for the management of large-break loss of coolant accident. *17th International Topical Meeting on Nuclear Reactor Thermal Hydraulics (NURETH-17)*, 2017.

[3] V.K. Saul'ev. On the solution of some boundary value problems on high performance computers by fictitious domain method. *Siberian Math. Journal*, 4(4) :912–925, 1963 (in Russian).

[4] C. Introïni, M. Belliard, and C. Fournier. A second order penalized direct forcing for hybrid cartesian/immersed boundary flow simulations. *Computers Fluids*, 90 :21–41, 2014.

[5] Michel Belliard and Clarisse Fournier. Penalized direct forcing and projection schemes for navier-stokes. *Comptes Rendus Mathematique*, 348, 10 2010.

[6] Charles-Henri Angot, Philippe ; Bruneau and Pierre Fabrie. A penalization method to take into account obstacles in incompressible viscous flows. *Numerische Mathematik*, 37(1) :239–261, 1999.

[7] J. Mohd-Yusof. Combined immersed-boundary/b-spline methods for simulations of flow in complex geometries. *Technical Report, NASA ARS/Stanford University CTR, Stanford.*, page 317–327, 1997.

[8] Tsutomu Ikeno and Takeo Kajishima. Finite-difference immersed boundary method consistent with wall conditions for incompressible turbulent flow simulations. *Journal of Computational Physics*, 226(2) :1485–1508, 2007.

[9] Georis Billo, Michel Belliard, and Pierre Sagaut. A finite element penalized direct forcing immersed boundary method for infinitely thin obstacles in a dilatable flow. *Computers Mathematics with Applications*, 99 :292–304, 2021.

[10] Lumley J.L. Tennekes, H. A first course in turbulence. *MIT Press*, 1994.

[11] Pierre Sagaut. Large eddy simulation for incompressible flows. *Springer ISBN : 978-3-540-26344-9*, 2006.

[12] S. Wilhelm, J. Jacob, and P. Sagaut. An explicit power-law-based wall model for lattice boltzmann method–reynolds-averaged numerical simulations of the flow around airfoils. *Physics of Fluids*, 30(6) :065111, 2018.

[13] Geneviève Comte-Bellot. Turbulent flow between two parallel walls. *Aeronautical Research Council*, 1969.

[14] H. Werner H. Wengle. Large-eddy simulation of turbulent flow over and around a cube in a plate channel. *Turbulent Shear Flows 8 pp 155–168*, 1993.